DESIGN OF AIRFOILS WITH HIGH LIFT AT LOW AND MEDIUM SUBSONIC MACHNUMBERS

by

F.X.Wortmann

Institut für Aerodynamik und Gasdynamik der Universität Stuttgart

Summary

The highlift capabilities of airfoils are restricted by the boundary layer separation on the upper airfoil surface. Therefore it is obviously desireable to design airfoils with pressure distributions which shift the onset of separation to higher angles of attack. In doing this the topside nose region becomes more and more important, not only with respect to the maximum lift but also for post-stall behaviour. Fortunately the nose region, especially with cambered airfoils, is to some extent free for modifications which do not necessary injury the airfoil drag qualities at low incidences i.e. at high speeds.

As long as the Machnumber stays below, say, .2 the design task on the one hand strives for lower velocity peaks at the nose insofar as this is compatible with the high speed requirements, and on the other hand for reduced velocity gradients behind the peak in the first 4-10% of the chord to produce turbulence without a pronounced laminar separation bubble. In other words, one aims for more favorable initial conditions for the turbulent boundary layer while at the same time avoiding the critical bursting of the separation bubble.

At higher Machnumbers and high angles of attack local supersonic fields will soon develop which are usually terminated by a shock. The best boundary layer control in this case is to avoid the shock by an appropriate design of the airfoil nose for a given angle of attack and Machnumber. The resulting form of the airfoil nose for shockless flow turns out to be quite near to the optimum form produced by the first design task, which takes into account only boundary layer considerations. Therefore it can be expected that an airfoil designed for high lift at a certain Machnumber say .5, will have excellent high lift values not only at this but also at lower Machnumbers, down to the incompressible case.

The common feature of these airfoils is a slight second peak in the curvature at 4 - 10% of the chord. The effectivity of this "hump" to increase the $C_{L\ max}$ will be shown by experimental results.

1. Introduction

The maximum lift of an airfoil and its stall behaviour are important qualities of any airfoil. They are strongly influenced by details of the boundary layer development and obviously any airfoil through its form and pressure distribution exerts some sort of boundary layer control.

It is now an interesting question to see what can be gained with respect to the maximum lift if the form of the airfoil is designed to produce the desired boundary layer control for a specific value of the Reynolds- and Machnumbers.

Since the underlying concepts are by no means new it is the purpose of this paper to illustrate the expected improvements by some experimental results.

2. High lift at low Machnumbers

At higher angles of attack all airfoils develop a small "laminar" separation bubble on the upper side near the leading edge, even at high Reynoldsnumbers. This separation has a strong and well-known influence on the maximum lift. The most striking feature of this tiny bubble is the ability to break up and burst into a big separated region. For thin airfoils this happens early, and due to the relatively low incidences the separated turbulent layer will soon reattach.

With increasing incidences the lift and the bubble grow until the reattachment line reaches the trailing edge. The maximum lift is moderate and the "thin airfoil" stall is steady.
With airfoils of medium thickness the length of the laminar separation bubble will be reduced with increasing incidences and reaches the break up condition only at high angles of attack.
A steady transition is now impossible. The bursting of the bubble causes completely separated flow and a sudden and significant loss of lift. This characterizes the leading edge stall.

With thicker airfoils the separation of the turbulent boundary layer in front of the trailing edge prevails and the stall will be reached before the laminar separation bubble at the nose becomes critical. The trailing edge stall may be more or less steady depending on how fast the separation point of the turbulent boundary layer moves forward. Even in this case the tiny laminar separation bubble has its effect; due to the large pressure differences and the type of pressure distributions associated with high angles of attack, the turbulent boundary layer becomes more and more sensitive to the initial conditions and without doubt the laminar separation bubble at the nose has a strong and detrimental influence on the turbulent boundary layer [1].

Thus it may be interesting to design airfoils with little or no laminar separation and to see if it is possible to increase the maximum lift or to change the type of stall. With respect to the laminar boundary layer this means locally reduced pressure gradients in the nose region and a shift of the separation point behind the transition point.

The chord length necessary to provoke the transition shortens with increasing Reynoldsnumber. On the other hand, speaking in terms of airfoil design it is easier to change the pressure gradients over a short rather than an extended chord length. Therefore the full benefits of this old concept [2] can be expected rather at higher Reynoldsnumber, say above $6 \cdot 10^6$.

In the following two symmetrical airfoils, the NACA 0009 and 0012, have been chosen to demonstrate the value of a nose modification.
Figure 1 and 2 show the form, the potential velocity at $\alpha = 14^\circ$ and the curvature of these airfoils and their modifications. The windtunnel tests were restricted to a Machnumber of .2 and a Reynoldsnumber of $3 \cdot 10^6$ to avoid any sonic velocities to within a fair margin.
Figure 3 shows the laminar separation bubbles of the 0012 and the FX 71-120 airfoil at 14° and 16,6° respectively, i.e. nearly one degree below $C_{L\ max}$.*)

Despite the longer laminar flow of the modified airfoils with adverse pressure gradients, the Reynoldsnumber is not high enough to avoid the separation bubble completely. It may be argued however that in this case the height of the separation bubble, and therefore the initial thickness of the turbulent boundary layer, is far less than with the 0012 airfoil.
Figures 4 and 5 give the lift and drag value of both the NACA airfoils and their modifications, and Figure 6 the $C_{L\ max}$ values as function of the Reynoldsnumber.**)
The modified airfoils exhibit a gain in $C_{L\ max}$ of 15 - 20% and increase the associated angle of attack by 2 or 3 degrees.
In both cases the stall of the modified airfoils has been changed to a trailing edge stall. The steep loss of lift beyond the stall could probably be moderated if the modifications were extended over the rear part of the airfoils. There is, however, at low incidences a drag penalty of 5 to 15% for the smooth airfoils due to the earlier transition on the modified versions. If the transition were enforced by some roughness at nearly 5% - 7% of the chord, the drag penalty would diminish.
The coordinates of the modified airfoils are given in Table I.

It may be mentioned that symmetrical airfoils are in some sense the hardest example with which to demonstrate the effectivity of a bubble control. For cambered airfoils there exists a greater degree of freedom do "hide" the modifications into the nose camber, and to avoid the drag penalty even with smooth airfoils.

3. High lift at medium Machnumbers

The high lift which an airfoil may attain at low Machnumbers will always decline when the Machnumber increases and the velocity peaks near the leading edge form a local supersonic field which is usually terminated by a more or less pronounced shock. The shock interference in turn hits a boundary layer, which in any case is already exhausted by the large pressure differences at high incidences.

It is thus not too surprising to find a pronounced depression in the envelope of the maximum lift curves in the Machnumber range between .3 and .55 [4]. This Machnumber range is of relevance especially to the helicopter rotor, which needs a high lift on the retreating blade to balance the disk loading in forward flight.

---

*) In these tests the tunnel speed accelerated in 30 sec from zero to Re = 3×10^6. Therefore in details the oil streak pattern needs some cautious interpretation.

**) All measurements were done by Dipl.-Phys. D.Althaus in the laminar wind tunnel of the institute [3].

In order to retain the high lift in the low to medium Machnumber range, it will be mandatory to design the upper nose region of the airfoil for a specifically chosen Machnumber and a certain high angle of attack. Similarly to the incompressible case, one must first reduce the velocity peaks by thickness and camber distribution as far as is compatible with the high speed requirements. The second design principle strives for an isentropic recompression in the supersonic field to reduce the strength of the terminating shock [5]. The recompression which may be achieved on the basis of the "peaky" concept or an analysis of the expansion and compression waves inside the supersonic field ensures at the same time that the residual shock in off-design conditions never interferes with a laminar boundary layer.

In a previous paper [6] the author has shown that at high incidences the pressure at the crest has a strong relationship to the point at which the maximum lift eventually recovers with increasing Machnumbers, and reaches a second maximum.

This pressure must be sufficiently low (or in other words the speed in the crest region must be higher than usual) to be of any value for Machnumbers between .3 and .55. Figure 7 gives an example of an airfoil designed for an improved maximum lift at $M_\infty = .5$. Disregarding the chord position the nose form, the incompressible potential velocity and the curvature distribution resemble the features which are typical for the airfoils in the first part of this paper.
Figure 8 illustrates the expansion and compression waves in the supersonic field of this airfoil for $\alpha = 9.8^\circ$, at two Machnumbers near .5. The necessary compressible potential velocity distributions were calculated on the basis of the NLR formula [7].
In Figure 9 and 10 experimental results are evaluated*). Figure 9 shows for a constant angle of attack of 11° the development of the local Machnumber on the upper nose region of the FX 69-H-098 airfoil. The extremely high peaks of local Machnumbers right at the nose indicate clearly the favorable effects of a partly isentropic recompression. This is again demonstrated in Figure 10, where the overall maximum lift is given as a function of the Machnumber.

Since this paper concentrates on $C_{L\ max}$, however one should not lose sight of the complete problem, which includes the high speed properties of the airfoil.
The high velocities in the 10% chord region, which yield the typical curvature distribution of Figure 7 are compatible with the low pitching moments desirable for any rotor blade.
It may be fair to state the drag divergence at high Machnumbers and low incidences compares well with other airfoils, at least for the airfoil presented here.

With respect to helicopter airfoils it would certainly be necessary to apply the concept of local supersonic flow with isentropic recompression not only to the high lift case of an airfoil but to its low lift properties as well. This challenging problem would seem to be solvable, and windtunnel tests are under way to prove the potential advantages of such airfoils, optimized for two differing conditions.

4. Conclusion

It has been shown by experimental results that the maximum lift of a symmetrical airfoil at low Machnumbers can be increased by some 15 to 20% if the airfoil nose is slightly modified and designed to yield lower velocity peaks and less pronounced laminar separation bubbles.
A similar improvement for the maximum lift at medium Machnumbers is possible if the upper nose region of the airfoil is designed to produce a "peaky" configuration at a certain Machnumber and high angle of attack. In both cases the airfoil exhibits as a common feature a high curvature or even a slight second peak in the curvature distribution between 4 to 10% of the chord.

References

[1] F.X. Wortmann
"Experimentelle Untersuchungen an neuen Laminarprofilen für Segelflugzeuge und Hubschrauber"
Zeitschrift f. Flugwiss. 5 (1957) S. 228-243

[2] F.X.Wortmann
"Progress in the design of Low Drag Airofoils"
"Boundary Layer and Flow Control" Pergamon Press London 1961, p. 748-770

*) These tests were done in the UAC-windtunnel (Hartford, Conneticut, USA) and were part of a research programm of the Bell Helicopter Co., Fort Worth, Texas.
I am grateful to this company for the permission to publish these data.

[3] F.X.Wortmann und D.Althaus
"Der Laminarwindkanal des Instituts für Aero- und Gasdynamik der TH Stuttgart"
Zeitschrift f. Flugwiss.12 (1964) S.129-134

[4] L.R.Wootton
The Effect of Compressibility on the Maximum Lift Coefficient of Airofoils at Subsonic Airspeeds
J.R.Aer.Soc.71 (1967), p.476

[5] H.H.Pearcy, J.Osborne
"Some Problems and Features of Transonic Aerodynamics
7.Congress of ICAS (1970), Rom

[6] F.X.Wortmann, J.M.Drees
Design of Airfoils for Rotors
CAL/AVLABS Symposium 1969, Cornell Aeron.La. Buffalo

[7] Th. E.Labrujere, W.Loeve, J.W.Slooff
"An approximate Method for the Determination of the Pressure Distribution on Wings in the lower Critical Speed Range"
AGARD CP Nr.35 (1968) Paris.

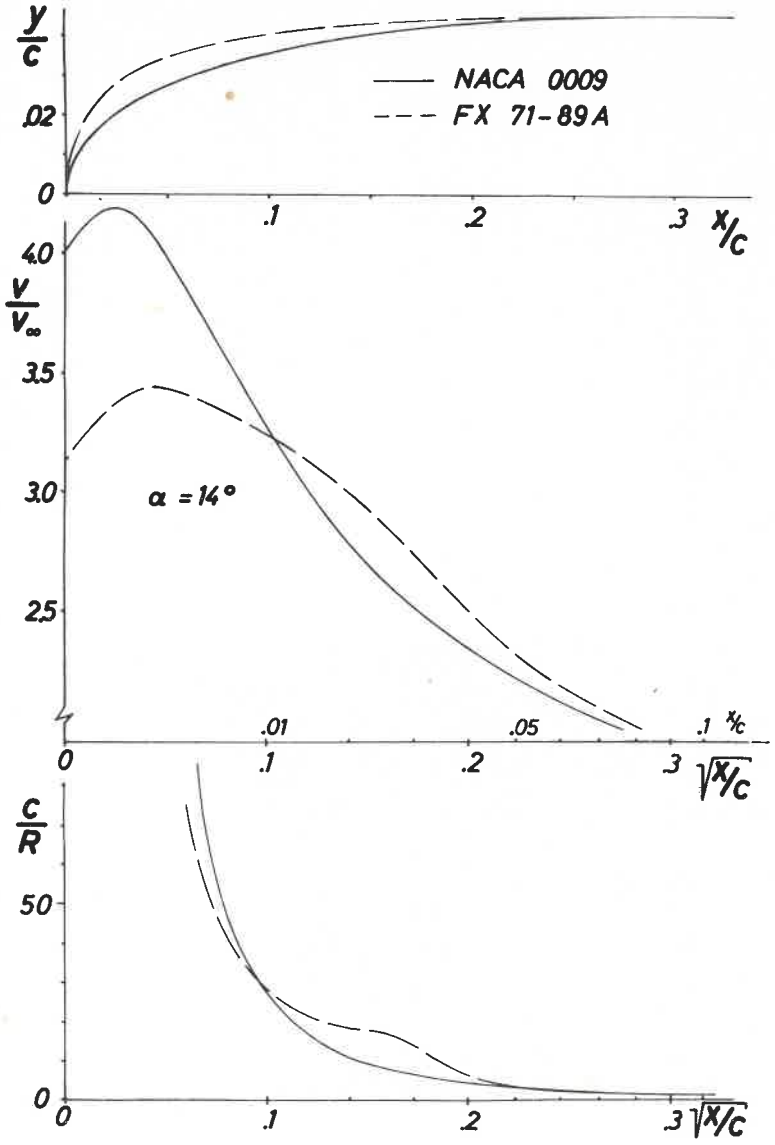

Fig.1 Form of airfoil nose, inviscid velocity distribution at $\alpha = 14^{o}$ and curvature distribution for the NACA 0009 and the FX 71-89A.

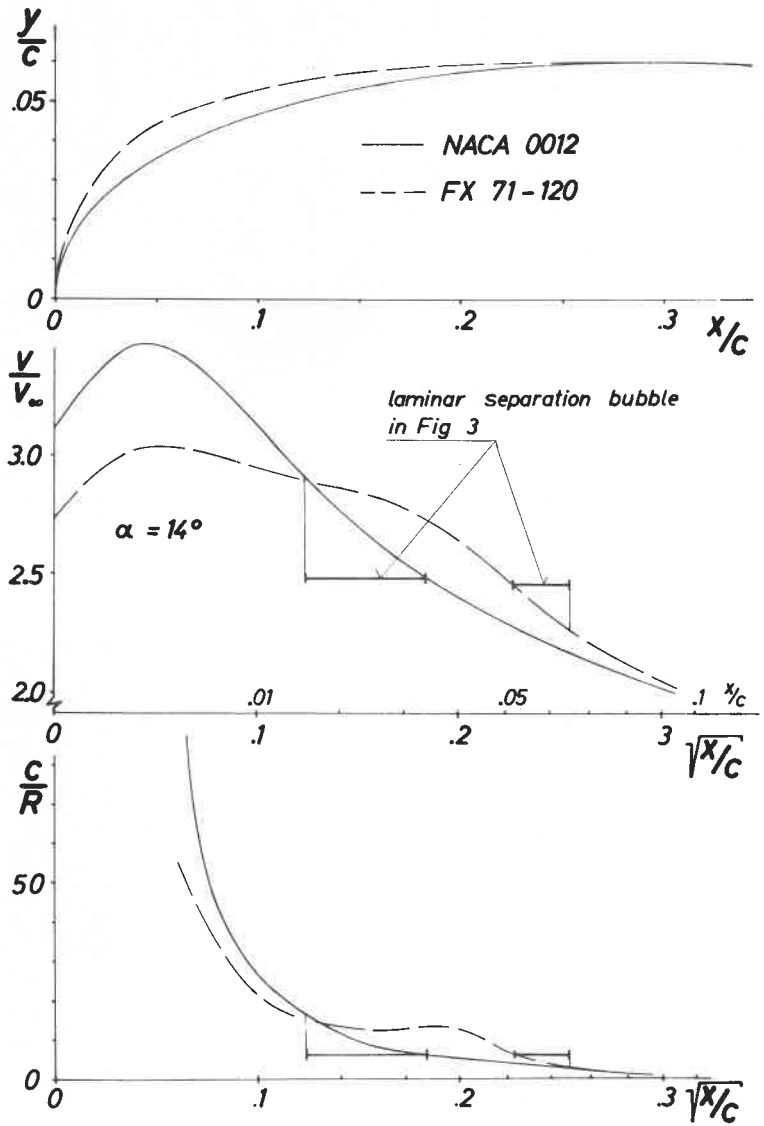

Fig.2 Form of airfoil nose, inviscid velocity distribution at $\alpha = 14^{o}$ and curvature distribution for the NACA 0012 and the FX 71-120

Table I

Airfoil coordinates given in per cent of airfoil chord

No.	x/c	FX 71-120 y/c	FX 71-089A y/c
4	.99039	.00093	.00088
6	.97347	.00344	.00257
8	.94844	.00655	.00487
10	.91573	.01037	.00769
12	.87592	.01493	.01107
13	.85355	.01745	.01295
14	.82967	.02011	.01491
15	.80436	.02293	.01701
16	.77779	.02586	.01912
17	.75000	.02879	.02133
18	.72114	.03179	.02356
19	.69134	.03478	.02578
20	.66072	.03771	.02794
21	.62941	.04053	.03005
22	.59755	.04331	.03209
23	.56526	.04595	.03406
24	.53270	.04836	.03586
25	.50000	.05072	.03763
26	.46730	.05275	.03915
27	.43474	.05466	.04057
28	.40245	.05627	.04179
29	.37059	.05760	.04280
30	.33928	.05862	.04359
31	.30866	.05937	.04416
32	.27886	.05983	.04456
33	.25000	.05993	.04467
34	.22221	.05980	.04466
35	.19562	.05931	.04435
36	.17033	.05833	.04376
37	.14645	.05708	.04291
38	.12408	.05531	.04171
39	.10332	.05323	.04037
40	.08427	.05072	.03865
41	.06699	.04786	.03646
42	.05156	.04443	.03411
43	.03806	.04069	.03118
44	.02653	.03486	.02818
45	.01704	.02812	.02341
46	.00961	.02118	.01804
47	.00428	.01408	.01220
48	.00107	.00714	.00630

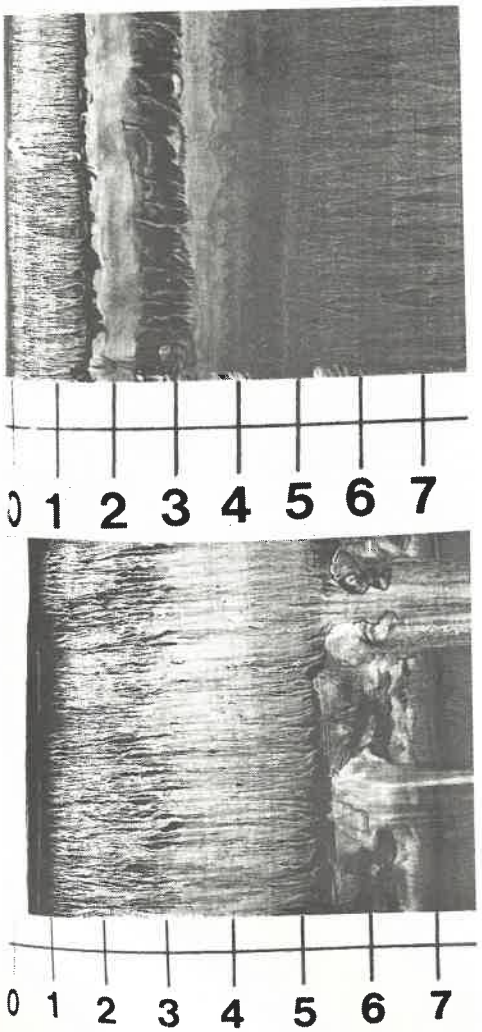

Fig.3 Oil film pattern of the NACA 0012 at $\alpha = 14^{\circ}$ (upper part) and of the FX 71-120 at $\alpha = 16.6^{\circ}$ (lower part), indicating the laminar separation bubble. Scale in per cent of airfoil chord.

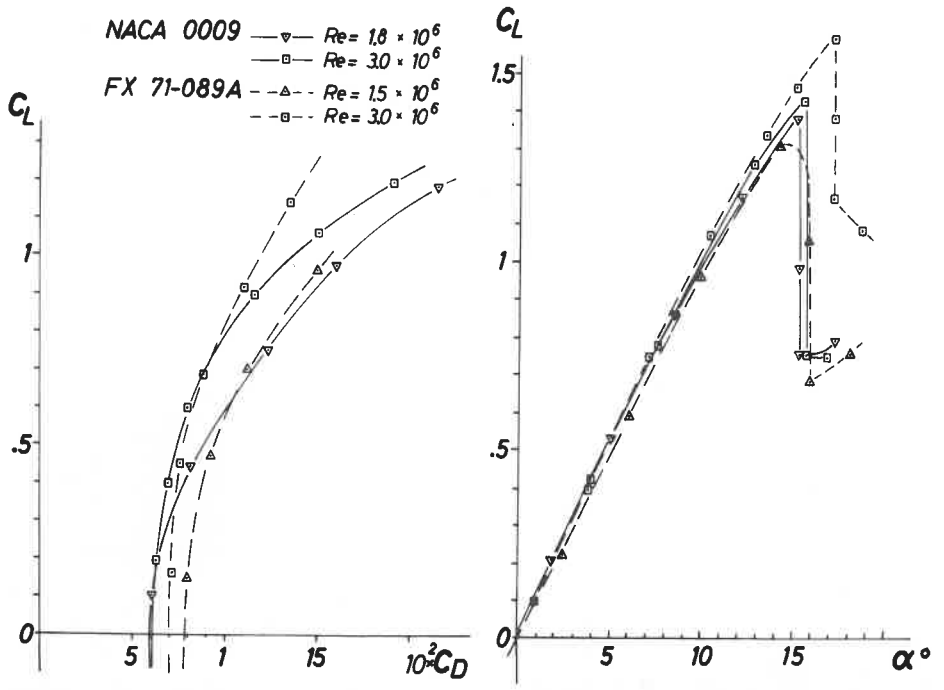

Fig.4: Experimental aerodynamic characteristics of the NACA 0009 and FX 71-089A for Reynoldsnumbers between $1.5 \cdot 10^6$ and $3 \cdot 10^6$.

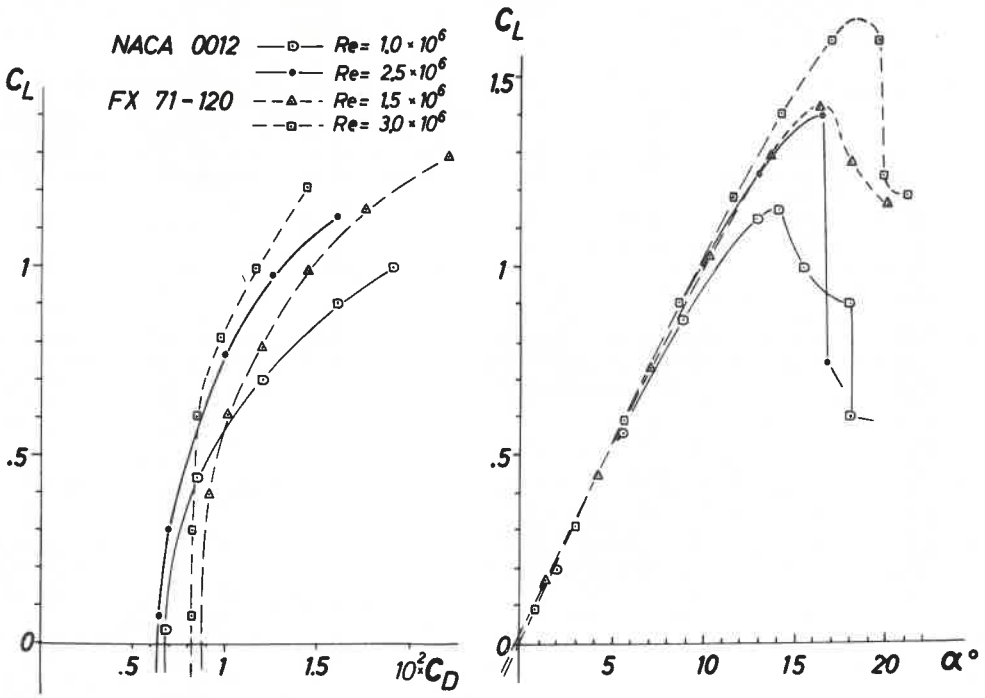

Fig.5: Experimental aerodynamic characteristics of the NACA 0012 and FX 71-120 for Reynoldsnumbers between $1 \cdot 10^6$ and $3 \cdot 10^6$.

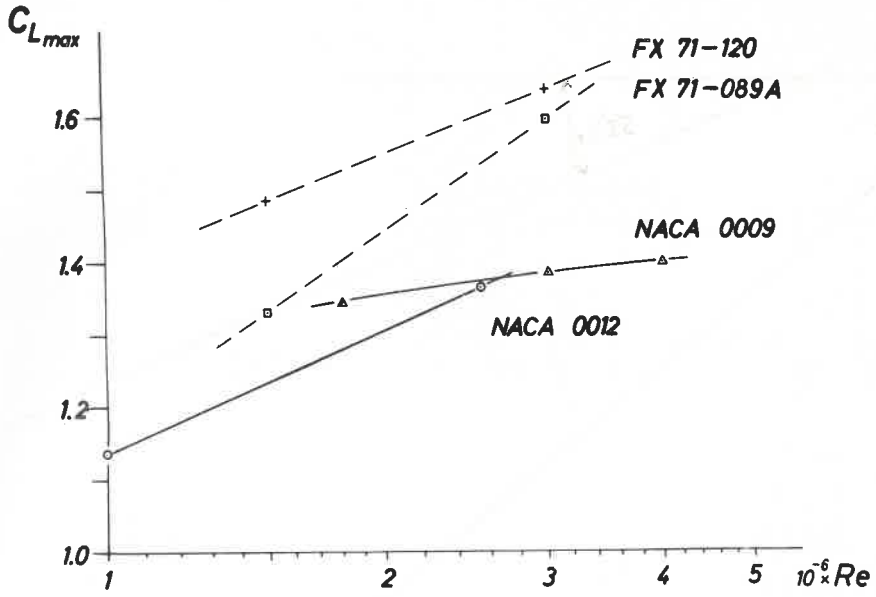

Fig.6: Variation of maximum lift coefficient with Reynoldsnumber for two NACA airfoils and their modifications.

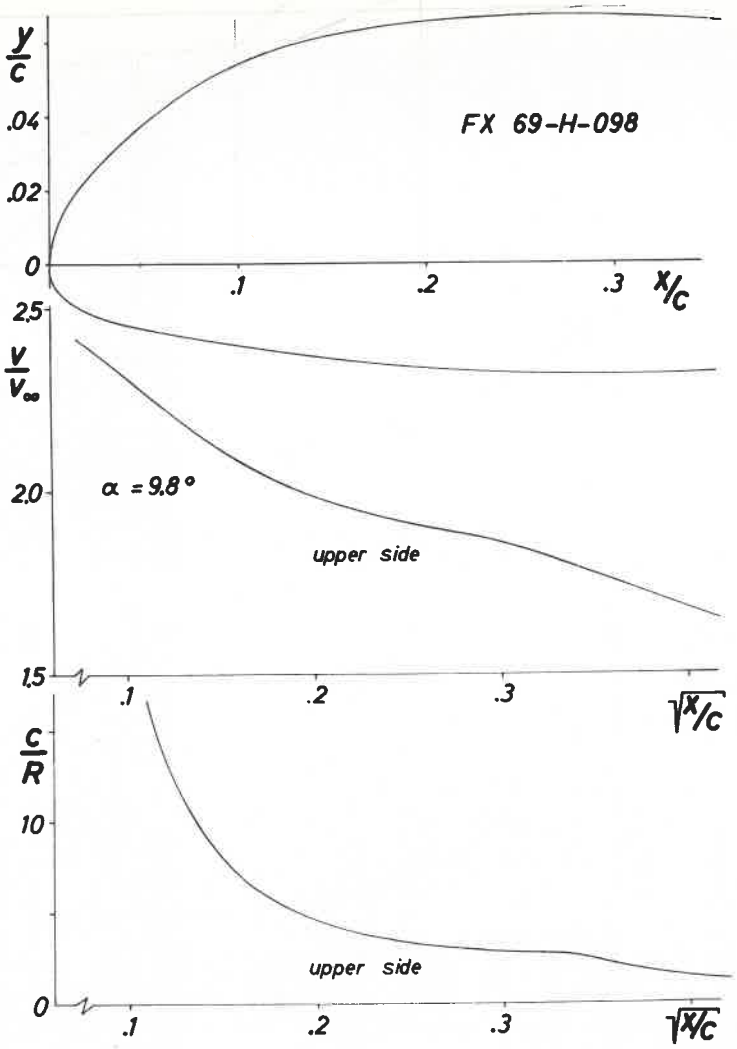

Fig.7: Form of airfoil nose, inviscid and incompressible velocity distribution at $\alpha = 9.8^{\circ}$ and curvature distribution on the upper side of FX 69-H-098.

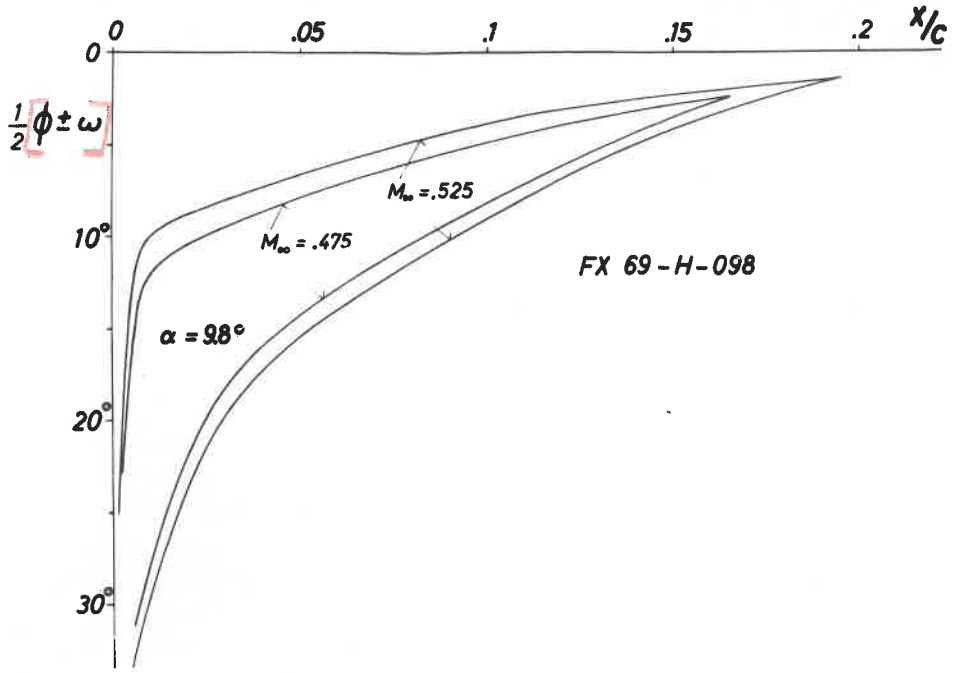

Fig.8: Wave cancellation analysis for FX 69-H-098 at $\alpha = 9.8^{\circ}$ and two Machnumbers.

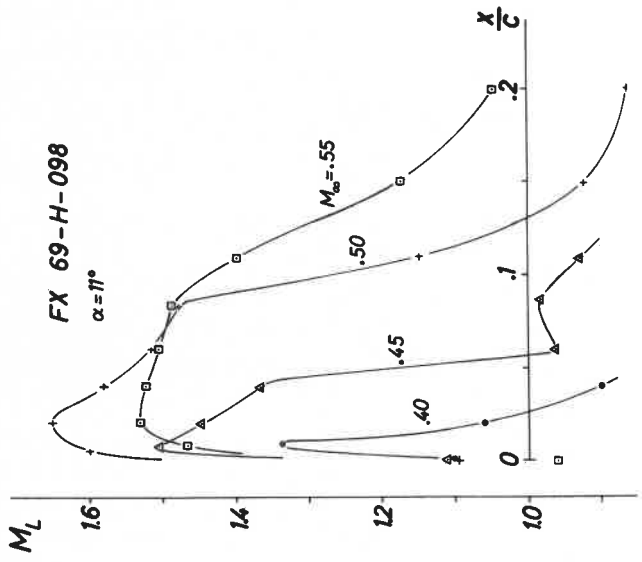

Fig. 9: Variation of local Machnumbers in the upper nose region of FX 69-H-098 at $\alpha = 11^{\circ}$ for free stream Machnumbers between .4 to .55. UAC-windtunnel.

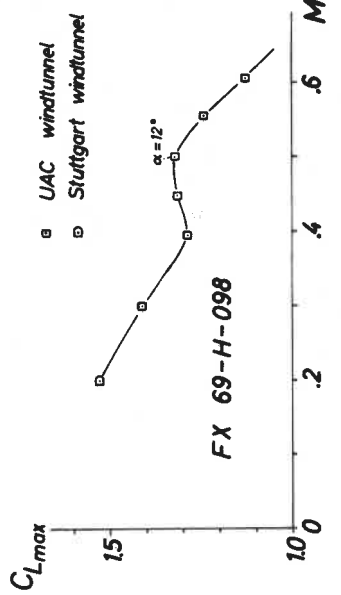

Fig.10: Variation of maximum lift coefficient at low and medium free stream Machnumber for the FX 69-H-098.